JACS
JOURNAL OF THE AMERICAN CHEMICAL SOCIETY

ARTICLE

pubs.acs.org/JACS

# Supramolecular Self-Assembly of Amphiphilic Anionic Platinum(II) Complexes: A Correlation between Spectroscopic and Morphological Properties

Charlotte Po, Anthony Yiu-Yan Tam, Keith Man-Chung Wong, and Vivian Wing-Wah Yam*

Institute of Molecular Functional Materials (Areas of Excellence Scheme, University Grants Committee (Hong Kong)) and Department of Chemistry, The University of Hong Kong, Pokfulam Road, Hong Kong

Supporting Information

**ABSTRACT:** A new class of amphiphilic anionic platinum(II) bzimpy complexes has been demonstrated to show aggregation in water through Pt···Pt and $\pi-\pi$ stacking interactions. An interesting aggregation−partial deaggregation−aggregation process and a morphological transformation from vesicles to nanofibers have been demonstrated. These changes can be systematically controlled by the variation of solvent composition and could readily be probed by UV−vis absorption, emission, NMR, transmission electron microscopy, and even with our naked eyes.

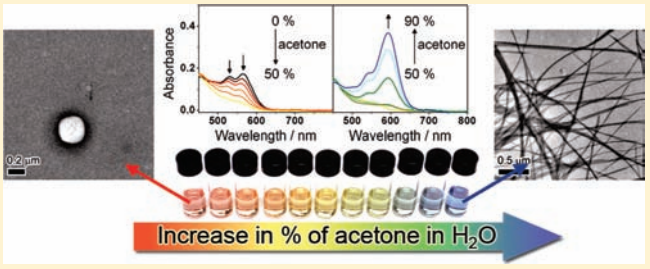


## INTRODUCTION

Luminescent square-planar $d^8$ metal polypyridyl complexes have attracted much attention due to their intriguing spectroscopic and luminescence properties, as well as their tendency to form metal−metal and $\pi-\pi$ stacking interactions.[1−9] While most of the studies on metal−metal and $\pi-\pi$ stacking interactions in platinum(II) system were related to solid-state polymorphism, it was only recently that we reported a cationic alkynylplatinum(II) terpyridyl complex, [Pt(tpy)(C≡C−C≡CH)]OTf (tpy = terpyridine), that showed drastic color changes in solutions upon a change in the composition of solvents due to metal−metal and $\pi-\pi$ interactions associated with aggregate formation.[5] Unlike the well-known oligomerization of $[Rh(CNR)_4]^+$ that occurred upon an increase in concentration in acetonitrile,[10] the aggregate formation in [Pt(tpy)(C≡C−C≡CH)]OTf was induced by reduced solvation upon an increase in the content of nonsolvent. Extension of the work to the design and synthesis of cationic alkynylplatinum(II) terpyridyl complexes that exhibited aggregation processes through Pt···Pt and $\pi-\pi$ stacking interactions in response to external stimuli such as temperature,[6,7] metallogel formation,[7] micelle formation,[8a] addition of anionic polymers,[8b,c] glucose-responsive polymers,[8d] biopolymers[9] and G-quadruplex formation,[9b,c] which led to the observation of drastic color changes and/or luminescence enhancement, has been reported. Recently, another class of cationic platinum(II) complexes with bzimpy as the *N*-donor ligand (bzimpy =2,6-bis(benzimidazol-2′-yl)pyridine) was also reported to show interesting vapochromic,[11] Langmuir−Blodgett,[12] thermochromic, and metallogel properties,[13] associated with the formation of Pt···Pt and $\pi-\pi$ stacking interactions.

Supramolecular chemistry represents a very important area in a number of research fields, such as chemistry, biology, and material science, mainly owing to its relevance to assembly from randomly oriented molecules to highly ordered supramolecular structures through a delicate balance of noncovalent interactions.[14] Among them, assemblies of amphiphilic molecules have attracted much attention due to their ability to form highly ordered aggregates with interesting morphology in solution such as micelles, vesicles, and fibers via differential interaction of the hydrophilic and hydrophobic moieties with the solvent.[15−19] Amphiphilic polymers which form vesicles have been examined for their potential applications in drug delivery and model systems of biomembranes,[17] while amphiphiles with organic chromophoric dyes were investigated to construct highly ordered nanostructured materials for optoelectronic applications.[14c,18f,18g] While most of the works have been focused on the study of amphiphilic polymers and amphiphiles with organic chromophoric dyes,[15−19] amphiphilic transition metal complexes are relatively less explored.[7,8,12,13,20,21] Owing to the rich spectroscopic and luminescence properties of square-planar $d^8$ platinum(II) complexes with tridentate *N*-donor ligand associated with the formation of Pt···Pt and $\pi-\pi$ stacking interactions, it is envisaged that amphiphilic platinum(II) complexes could serve as a versatile reporter to probe the formation of supramolecular assemblies. These, together with the lack of reports on the aggregation of anionic platinum(II) complexes, have prompted us to explore amphiphilic anionic platinum(II) bzimpy complexes and to study the correlation between the morphological transformations and spectroscopic changes. Herein, we report the synthesis of amphiphilic anionic platinum(II) bzimpy complexes (Scheme 1) and their interesting spectroscopic and luminescence changes upon a

**Received:** April 28, 2011
**Published:** July 20, 2011





dx.doi.org/10.1021/ja203920w | *J. Am. Chem. Soc.* 2011, 133, 12136–12143

**Scheme 1. Structures of the Amphiphilic Anionic Platinum(II) bzimpy Complexes**

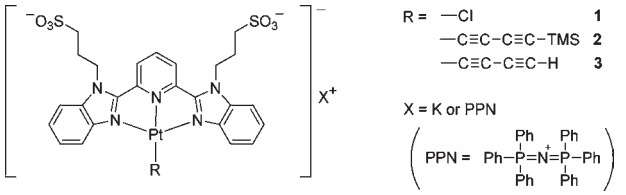


variation of the solvent composition; such changes were found to be associated with their morphological transformation.

## RESULTS AND DISCUSSION

Amphiphilic platinum(II) complex **1** in potassium salt (**1**·K) was prepared by the reaction of $K_2PtCl_4$ with the sulfonate-pendant bzimpy ligand in DMSO. Due to the low solubility of **1**·K in common organic solvents which made the incorporation of the alkynyl ligands difficult, its PPN salt, **1**·PPN (PPN = bis(triphenylphosphine)iminium), was prepared by the metathesis reaction in the presence of PPNCl in water. Further reaction of complex **1**·PPN with TMS−C≡C−C≡CH in dichloromethane in the presence of tri-*n*-octylamine and a catalytic amount of copper(I) iodide yielded the platinum(II) alkynyl complex **2**, and metathesis reaction with $KPF_6$ afforded **2**·K in almost quantitative yield. The deprotection of the trimethylsilyl group of **2**·K under basic condition by potassium carbonate in water gave **3**·K. All the complexes can be purified simply by the interconversion between the corresponding potassium and PPN salts and have been characterized by $^1$H NMR spectroscopy, negative FAB mass spectrometry, IR spectroscopy, and satisfactory elemental analyses.

It is interesting to note that two solid forms of **1**·K, the yellow form and the deep-blue form, could be isolated. In their solid state UV−vis absorption spectra, a low-energy absorption band at 613 nm was observed in the deep-blue form that imparts its blue color, which was absent in the yellow form (Figure 1). On the basis of the spectroscopic studies of the different crystal forms of the related platinum(II) systems, such as $[Pt(bpy)Cl_2]$,[2] $[Pt(terpy)Cl]^+$,[3c] $[Pt(terpy)(C{\equiv}CR)]^+$ [5] and $[Pt(bzimpy)Cl]^+$,[11] such low-energy absorption band at 613 nm in the deep-blue form is tentatively assigned as the metal−metal-to-ligand charge transfer (MMLCT) [$d\sigma^*(Pt)\rightarrow\pi^*$(bzimpy)] transition, associated with the formation of Pt···Pt and $\pi-\pi$ stacking interactions. Upon photoexcitation at $\lambda$ > 400 nm, complexes **1**·K (both the yellow and deep-blue forms), **2**·K and **3**·K were found to give intense emission in the solid state at 298 and 77 K, and the photophysical data are tabulated in Table 1. Except for the yellow form of **1**·K which showed vibronic-structured triplet intraligand ($^3$IL) [$\pi\rightarrow\pi^*$(bzimpy)] emission at 551 nm, typical of emission found in the monomeric complexes,[11−13] all the complexes gave low-energy, structureless emission bands at 679−711 nm, which were assigned as originating from triplet metal−metal-to-ligand charge transfer ($^3$MMLCT) excited state.[11−13] A red shift of such a low-energy emission band was observed at the low temperature of 77 K due to the possible enhancement of Pt···Pt and $\pi-\pi$ stacking interactions as a result of the lattice contraction upon cooling.

Dissolution of the potassium salts of complexes **1**−**3** in aqueous solutions gave red or orange solutions at room temperature. The electronic absorption spectra of the potassium salts

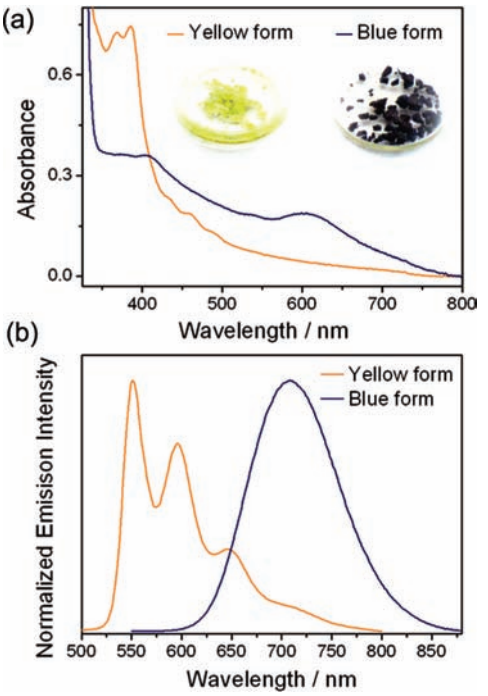


**Figure 1.** (a) Solid-state UV−vis absorption spectra and (b) normalized emission spectra of **1**·K in yellow and blue forms at room temperature.

of complexes **1**−**3** in water at 298 K showed very intense intraligand (IL) [$\pi\rightarrow\pi^*$(bzimpy)] absorptions at ~312−358 nm and less intense absorption tails at ~434 nm (Table 1 and Figure 2a). The low-energy absorption tails are assigned as metal-to-ligand charge transfer (MLCT) [$d\pi$(Pt)$\rightarrow\pi^*$(bzimpy)] transitions, with probably ligand-to-ligand charge transfer (LLCT) [$\pi$(C≡C)$\rightarrow\pi^*$(bzimpy)] character also involved in complexes **2**·K and **3**·K. For complexes **1**·K and **3**·K, additional absorption bands were observed at ~522−564 nm, which were less obvious in complex **2**·K, assignable to the spin-allowed metal−metal-to-ligand charge transfer (MMLCT) transitions, associated with Pt···Pt and $\pi-\pi$ stacking interactions. Upon photoexcitation at $\lambda$ > 400 nm, **1**·K−**3**·K in aqueous solutions showed low-energy structureless emission bands at ~675−683 nm. The close resemblance of the excitation spectra monitored at these emission bands with the low-energy absorption bands at 522−564 nm observed in the corresponding UV−vis absorption studies in water indicated that they are derived from the same origin and are assigned as $^3$MMLCT emission.

Interestingly, these low-energy absorption bands at ~522−564 nm were found to be highly sensitive to temperature, in which the absorption bands showed a drop in intensity and a blue shift in the absorption maxima with a concomitant growth of a high-energy absorption shoulder at ~440 nm with an isosbestic point at 460 nm upon increasing the temperature (Figure 3a). As the temperature is increased, the complex molecules are believed to undergo deaggregation processes with a weakening of the intermolecular Pt···Pt and $\pi-\pi$ stacking interactions; hence, a drop and blue shift of the MMLCT absorption bands are observed.[6,13] In the corresponding temperature-dependent emission studies with excitation at the isosbestic wavelength, a drop in the emission intensity and a blue shift in the emission maxima were observed for the $^3$MMLCT emission at ~675−683 nm. It is worthwhile to note that, while the low-energy MMLCT


dx.doi.org/10.1021/ja203920w |J. Am. Chem. Soc. 2011, 133, 12136–12143

**Table 1. Photophysical Properties of Platinum(II) bzimpy Complexes**

| complex | medium ($T$/K) | appearance | $\lambda_{abs}$/nm ( $\varepsilon$/mol$^{-1}$ dm$^3$ cm$^{-1}$) | $\lambda_{em}$/nm ($\tau_o$ / $\mu$s) | $\Phi_{lum}$ |
|---|---|---|---|---|---|
| **1**·K | water (298) | | 312 (19600), 338 sh (15100), 370 sh (11500), 422 (1890), 530 (1240), 564 (1350) | 683 (0.30) | 0.043 |
| | solid (298) | yellow | | 551 (0.62)[a] | |
| | solid (298) | deep-blue | | 711 (<0.1) | |
| | solid (77) | deep-blue | | 734 (1.78) | |
| **2**·K | water (298) | | 326 (20200), 358 sh (16900), 426 (3560), 520 (1030), 554 (705) | 678 (0.39) | 0.032 |
| | solid (298) | orange | | 685 (0.17) | |
| | solid (77) | | | 690 (2.14) | |
| **3**·K | water (298) | | 322 (19000), 346 sh (15900), 422 (2420), 522 (1430), 558 (1370) | 675 (0.45) | 0.111 |
| | solid (298) | red | | 679 (0.15) | |
| | solid (77) | | | 712 (1.56) | |

[a] Vibronic-structured emission band.

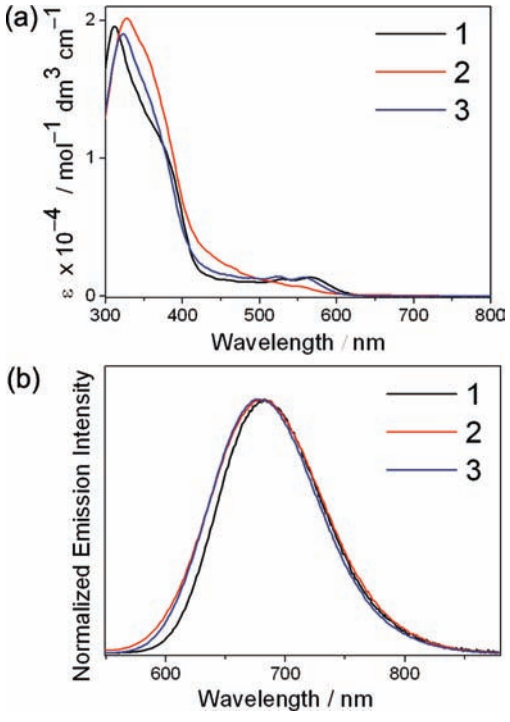


**Figure 2.** (a) UV−vis absorption spectra and (b) normalized emission spectra of of **1**−**3**·K in aqueous solutions at room temperature.

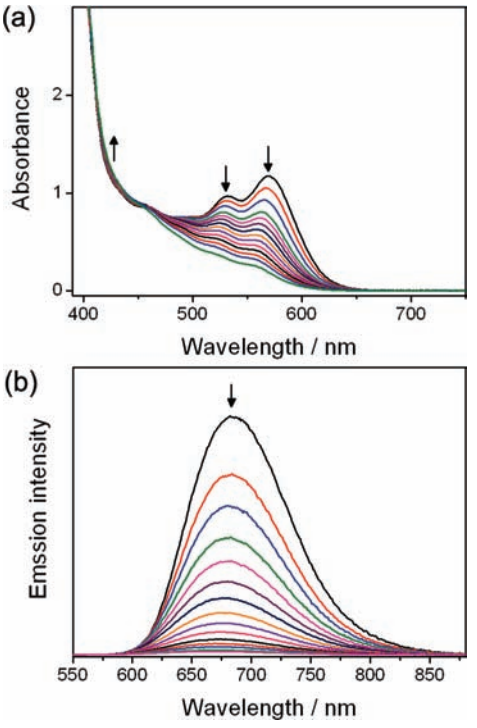


**Figure 3.** (a) UV−vis absorption spectra of **1**·K in water ([Pt] = 6.51 × 10$^{-4}$ M) upon increasing the temperature from 288 to 370 K. (b) Corrected emission spectra of the aqueous solution of **1**·K upon increasing the temperature from 288 to 370 K.

absorption and emission bands in **1**·K and **3**·K showed a decrease in intensity, they did not disappear completely even at 370 K, indicating that there is still a substantial extent of Pt···Pt and $\pi-\pi$ stacking interactions retained at such a high temperature. In order to quantify the degree of aggregation in aqueous solution, a dimerization plot for a monomer−dimer equilibrium[4a,c,d] for complex **1**·K monitored at 530 nm was performed, which gave a straight line plot in the concentration range of 2.05 × 10$^{-6}$ to 8.26 × 10$^{-3}$ M (Figure 4). From the plot, $K_{MM}$ and $K_{\pi\pi}$ values are found to be 8.2 × 10$^5$ M$^{-1}$ and 1.2 × 10$^5$ M$^{-1}$, respectively, which are much higher than those values reported for square-planar tetrakis(phenylisocyanide)rhodium(I) complexes[10,22] and platinum(II) polypyridyl complexes.[4a−d] These observations suggested that **1**·K showed a very high tendency toward aggregate formation through Pt···Pt and $\pi-\pi$ stacking interactions in solution even at room temperature without external stimuli.

Interestingly, **1**·K showed strong solvatochromic changes in water−acetone mixture. Upon the addition of acetone to the aqueous solution of **1**·K, the solution changed from red (100% water) to yellow (50% acetone−water) to blue (90% acetone) (Figure 5a). From the UV−vis absorption spectra of equimolar concentrations of **1**·K in different water−acetone compositions (Figure 5b), it was found that the MMLCT absorption bands at 532 and 564 nm for the red solution in 100% water dropped in absorbance upon increasing the acetone content to up to 50%, which resulted in the yellow-colored solution. On further addition of acetone, the yellow solution gradually turned blue through green with the appearance of new absorption bands at 542 and 594 nm. All the solutions remain stable for a week without precipitation, and the processes are fully reversible upon the evaporation of acetone. As in other platinum(II) polypyridyl

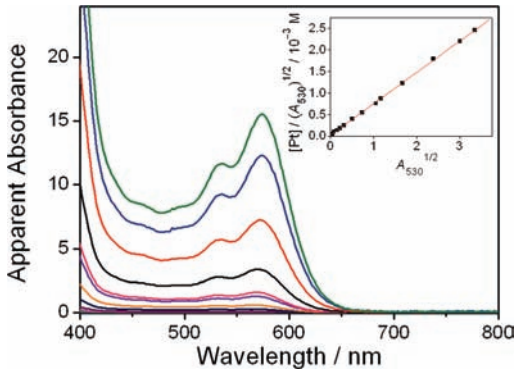


**Figure 4.** UV−vis absorption spectra of **1**·K in water in the concentration range of $2.05 \times 10^{-6}$ to $8.26 \times 10^{-3}$ M. The apparent absorbance values have been obtained by correcting to a 1-cm path length equivalence. (Inset) Dimerization plot for a monomer−dimer equilibrium for complex **1**·K in water monitored at 530 nm.

complexes, the dropping in absorbance but incomplete disappearance of the MMLCT absorption bands upon increasing the acetone content to up to 50% indicates the occurrence of a partial deaggregation process by dissociation of Pt···Pt and $\pi-\pi$ stacking interactions in 50% acetone−water. Surprisingly, in sharp contrast to the aggregation of platinum(II) polypyridyl complexes that only showed single aggregation−deaggregation processes, further addition of acetone to the **1**·K solution mixture gave rise to new MMLCT absorption bands at energies lower than those observed in 100% water, indicating the formation of a second aggregate species through Pt···Pt and $\pi-\pi$ stacking interactions. As it is well-known that stronger Pt···Pt and $\pi-\pi$ stacking interactions would lead to lower MMLCT energy, such red shifts in MMLCT absorption energy indicate that the second aggregate species is formed by stronger Pt···Pt and $\pi-\pi$ stacking interactions than that formed in water. The corresponding emission study of complex **1**·K was also performed. In its aqueous solution, a 683-nm structureless $^3$MMLCT emission band was observed. Upon increasing the acetone content in water and excitation at the isosbestic point, the emission band at 683 nm dropped in intensity, and a new emission band at slightly lower energy appeared (Figure 5c). Consistent with the UV−vis absorption study, this class of amphiphilic anionic platinum(II) complexes showed a cycle of aggregation−partial deaggregation−aggregation upon increasing the composition of acetone in water.

The aggregation−partial deaggregation−aggregation process is further supported by NMR spectroscopic studies. The $^1$H NMR spectra of **1**·K at different solvent compositions are shown in Figure 6. In $D_2O$, complex **1**·K showed very broad and poorly resolved NMR signals at 323 K, indicating that it would undergo self-assembly to form aggregate species.[6] In contrast, the bandwidth and the resolution of the NMR signals were found to improve and the chemical shift of the aromatic signals would show a downfield shift in 50% [$D_6$]-acetone−$D_2O$ mixture at the same concentration. Given the fact that the NMR signals were still not completely well resolved, a partial deaggregation process should have occurred (vide supra). However, a higher [$D_6$]-acetone content in $D_2O$ (90%) led to a very broad and almost featureless NMR spectrum, consistent with the corresponding UV−vis absorption study, where the formation of a second aggregate species with stronger interactions could be inferred.

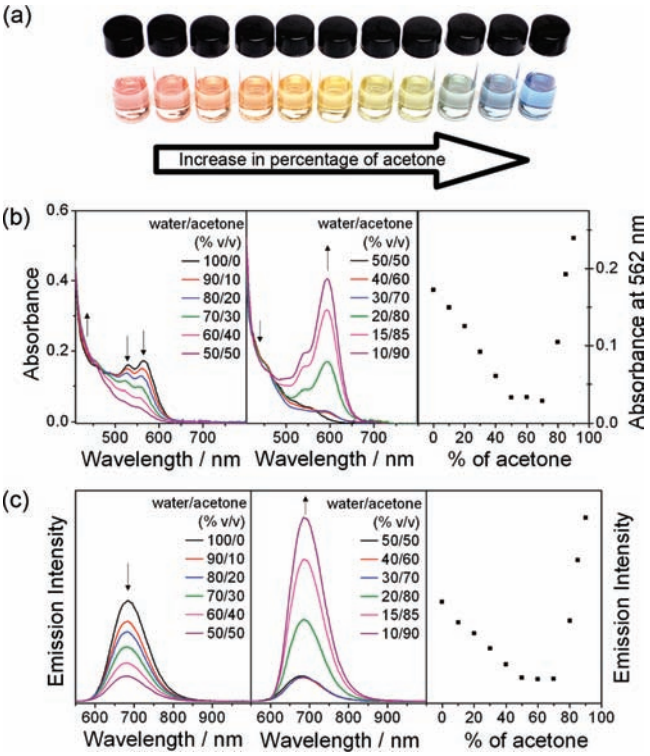


**Figure 5.** (a) Solutions of **1**·K in water−acetone mixture (percentage of acetone in water from left to right: 0, 10, 20, 30, 40, 50, 60, 70, 80, 85, 90%). (b) UV−vis absorption spectra of **1**·K ([Pt] = $1.37 \times 10^{-4}$ M) upon increasing the acetone content in water and plot of absorbance at 562 nm versus percentage of acetone. (c) Corrected emission spectra of **1**·K ([Pt] = $1.37 \times 10^{-4}$ M) upon increasing the acetone content in water and plot of emission intensity versus percentage of acetone.

Analogous to complex **1**·K, orange aqueous solutions of complex **3**·K turned to yellow and then to magenta (Figure S1a, Supporting Information [SI]) with similar UV−vis absorption and emission spectral changes (Figure S1b,c, SI) upon an increase in the acetone content. The less drastic color change may possibly be attributed to weaker Pt···Pt interactions under both aqueous and water−acetone media due to the presence of the hydrophobic alkynyl ligand. It is worth noting that **3**·K required more acetone (80%) than **1**·K (74%) to trigger the formation of the new MMLCT bands, suggesting that the presence of the hydrophobic alkynyl ligand would hinder the formation of the second aggregate species. However, with the incorporation of a bulky trimethylsilyl group in **2**·K, the second aggregation step was not observed. Upon increasing the acetone content, the solution was found to change from orange to yellow, and the MMLCT bands in both the UV−vis absorption and emission spectra dropped in intensity. No growth of a new band was observed in the absorption spectra, but a $^3$IL emission, typical of monomeric platinum(II) bzimpy complexes[11−13] was turned on when the percentage of acetone was increased to 70% (Figure S2a,b, SI). To further confirm the deaggregation process, $^1$H NMR experiments of **2**·K at various water−acetone compositions were performed. The broad NMR signals in 100% water became well resolved when the percentage of acetone was increased (Figure S3, SI). Unlike the spectra of **1**·K that showed only partial deaggregation, the NMR signals of **2**·K can be completely resolved at room temperature when the acetone composition is increased to 80%. These suggest that the formation

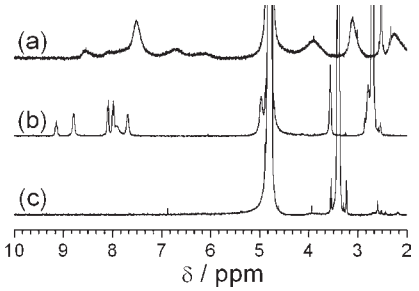


**Figure 6.** $^{1}$H NMR spectra of **1**·K in (a) $D_2O$, (b) 50% [$D_6$]-acetone−$D_2O$ and (c) 90% [$D_6$]-acetone−$D_2O$ at 323 K.

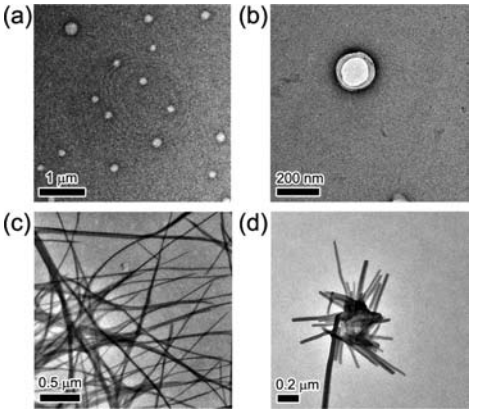


**Figure 7.** TEM images prepared from the aqueous solution of (a) **1**·K and (b) **3**·K. TEM images prepared from 90% acetone−water mixture of (c) **1**·K and (d) **3**·K.

of the second aggregate species would be difficult in the presence of bulky substitutents; thus, only deaggregation was observed with increased acetone composition.

In order to establish the identity of the first and second aggregate species in water and water−acetone mixture respectively, transmission electron microscopy (TEM) and scanning electron microscopy (SEM) were used to probe the morphological changes in various water−acetone compositions. The TEM images of **1**·K and **3**·K in aqueous solutions showed vesicles with diameters of about 200 nm (Figure 7a,b). The vesicles are probably made up of bilayer or multilayer structures as in other amphiphilic molecules.[15−19] Upon the addition of acetone, the aqueous solution of **1**·K turned blue with the observation of long nanofibers of about 20 nm thick and a few $\mu$m long in the TEM images (Figure 7c) and SEM images (Figure S4a, SI), while the magenta solution of **3**·K gave nanorods of about 30 nm thick and 1 $\mu$m long (Figures 7d and S4b [SI]). Confocal fluorescence microcopy was also utilized to examine the nanostructures in the 90% acetone−water mixture. Unlike TEM and SEM which require the sample in the dried state, confocal fluorescence microcopy allows the direct examination of the sample in solution. In both **1**·K and **3**·K, luminescent rods with dimensions of about 0.5 $\mu$m wide and a few $\mu$m long (Figure 8) showed an emission maximum at about 680 nm (Figure S5, SI) which is close to that observed in solution. A rod of slightly larger size than those observed in TEM is probably due to the shrinkage of the structures by loss of solvent during the drying process for TEM measurements. From the microscopy images and all other

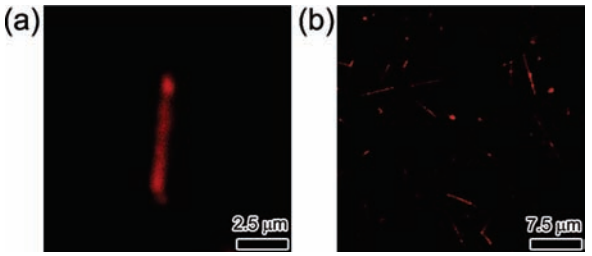


**Figure 8.** Confocal fluorescence microscopy images of (a) **1**·K and (b) **3**·K prepared from 90% acetone−water mixture.

spectroscopic changes observed, together with the consideration of the amphiphilicity of the complexes, possible mechanisms for the aggregation−partial deaggregation−aggregation process could be suggested. The anionic sulfonate head of the complex has a high affinity for water while the Pt(bzimpy) and the alkynyl moieties are more hydrophobic in nature. It is likely that, in water, the sulfonate groups would point toward water, while the Pt(bzimpy) moieties would be forced to pack together through Pt···Pt and $\pi-\pi$ stacking interactions in order to avoid unfavorable contact with water, to form the bilayered structures of the vesicles, giving rise to the poorly resolved NMR signals and the MMLCT absorption and emission bands. When more acetone is added, the Pt(bzimpy) moiety would be well solvated and the complex molecules would be more well dispersed, resulting in the drop of the MMLCT absorption and emission, as well as an improvement in the resolution of the NMR signals. As the acetone content is further increased, the sulfonate groups are no longer well solvated by the nonpolar solvent; thus, the sulfonate ionic heads would start to aggregate and pull the complexes into close proximity, leading to their aggregation through Pt···Pt and $\pi-\pi$ stacking interactions to form the nanofibers or nanorods, which are signaled by the development of the new MMLCT absorption and emission bands as well as the featureless NMR signals.

In order to investigate the aggregation−partial deaggregation−aggregation mechanism, UV−vis absorption studies of **1**·K in water−tetrahydrofuran (THF), water−ethanol, and water−acetonitrile (MeCN) were performed. Similar UV−vis absorption changes as that observed in the water−acetone mixture for the aggregation−partial deaggregation−aggregation phenomena were observed upon increasing nonaqueous solvent content (Figure S6, SI). It is interesting to note that the deaggregation process is highly dependent on the solubility of the complex in nonaqueous solvents as well as the nature of the solvent, as revealed by the observation that less acetonitrile (38%) is required to achieve saturation of partial deaggregation than acetone (50%) and THF (47%). This is probably attributed to the fact that **1**·K is more soluble in acetonitrile than THF and acetone, which would assist the partial deaggregation process upon the addition of acetonitrile since the Pt···Pt and $\pi-\pi$ stacking interactions in vesicles has to be destroyed by solvation of the Pt(bzimpy) moiety by nonaqueous solvents and also by disruption of the hydrogen bonding between water and the sulfonate groups. In the ethanol−water mixture, an exceptionally large amount of ethanol is needed to achieve saturation of the partial deaggregation process even though **1**·K is more soluble in ethanol than THF and acetone. This could be rationalized by the fact that similar to water, ethanol interacts with the sulfonate groups through hydrogen bond, which would

facilitate the alignment of the molecules for assembly.[23] Therefore, a competition between partial deaggregation and aggregation occurs upon the addition of ethanol. Further increase in the percentage of nonaqueous solvent would lead to the second aggregation, and the percentage of nonaqueous solvent to induce the second aggregation is lower in more hydrophobic solvents such as THF (71%) and acetone (74%) relative to polar acetonitrile (80%) and ethanol (80%). It is believed that more hydrophobic conditions would facilitate the aggregation of the sulfonate ionic heads and hence the formation of nanofiber or nanorod through stronger Pt···Pt and $\pi-\pi$ stacking interactions.

To conclude, we have demonstrated supramolecular self-assembly of a new class of amphiphilic anionic platinum(II) bzimpy complexes via aggregation of Pt···Pt and $\pi-\pi$ stacking interactions that can be systematically controlled by the variation of solvent composition. An interesting morphological transformation from vesicles to nanofibers has been demonstrated by transmission electron microscopy, and the corresponding spectroscopic and luminescence changes have been readily probed by UV−vis absorption, emission, NMR, and even with our naked eyes. It is envisaged that with its high water solubility and strongly emissive nature in water, together with its drastic emission and absorption changes on aggregation and deaggregation, this class of platinum(II) complexes may serve as ideal candidates which may be further explored for potential sensing or imaging purposes.

## EXPERIMENTAL SECTION

**Materials and Reagents.** Potassium tetrachloroplatinate(II) [$K_2PtCl_4$ (Chem. Pur., 98%)], 1,3-propanesultone (Alfa Aesar, 99%), tri-*n*-octylamine (ABCR, 98%), potassium hexafluorophosphate [$KPF_6$ (Sterm, 99.5%)], and bis(triphenylphosphine)iminium chloride [PPNCl (Sterm)] were purchased from the corresponding chemical company. 1-Trimethylsilyl-buta-1,3-diyne (TMS−C≡C−C≡CH)[24] and 2,6-bis-(benzimidazol-2′-yl)pyridine (bzimpy)[25] were prepared according to literature procedure. All other reagents and solvents were of analytical grade and were used as received.

**Synthesis.** *Synthesis of 2,6-Bis(1-(3-propylsufonate)benzimidazol-2′-yl)pyridine (**L1**).* To a hot mixture of 2,6-bis(benzimidazol-2′-yl) pyridine (2.00 g, 6.4 mmol), KOH (1.44 g, 25.7 mmol) and $^n$Bu$_4$NBr (0.14 g, 0.43 mmol) in DMSO (10 mL)/$H_2O$ (10 mL), was added dropwise a DMSO solution of 1,3-propanesultone (3.14 g, 25.7 mmol). The reaction was allowed to stir at 150 °C overnight. After removal of water under reduced pressure, acetone was added to precipitate out the product, which was collected by filtration to yield yellow solids. Yield: 3.80 g (94%). $^1$H NMR (400 MHz, [$D_6$]DMSO, 298 K): $\delta$ 1.99 (m, 2H, $CH_2$), 2.23 (t, $J$ = 7.4 Hz, 2H, $CH_2SO_3$), 4.93 (t, 2H, $J$ = 7.0 Hz, $CH_2N$), 7.28−7.38 (m, 4H, benzimidazolyl), 7.76−7.81 (m, 4H, benzimidazolyl), 8.22 (t, $J$ = 7.3 Hz, 1H, pyridyl), 8.35 ppm (d, $J$ = 7.9 Hz, 2H, pyridyl). Negative FAB MS: $m/z$ 554 [M−2K+H]$^-$, 592 [M−K]$^-$.

*Synthesis of **1**·K.* It was synthesized according to a modification of a literature procedure for the synthesis of chloroplatinum(II) bzimpy complexes.[12] **L1** (1.83 g, 2.89 mmol) and $K_2PtCl_4$ (0.80 g, 1.92 mmol) were heated in DMSO (10 mL) at 150 °C under a nitrogen atmosphere overnight to give a yellow suspension. Methanol and acetone were added to complete the precipitation of the product from the reaction mixture. After filtration, the yellow solid was washed with methanol and then acetone. The yellow solid is hygroscopic and turns blue in the presence of moisture. The blue solid was isolated for characterization. Yield: 0.91 g (57%). $^1$H NMR (400 MHz, [$D_6$]DMSO, 298 K): $\delta$ 2.18 (m, 2H, $CH_2$), 2.68 (t, $J$ = 6.0 Hz, 2H, $CH_2SO_3$), 4.90 (t, 2H, $J$ = 6.1 Hz, $CH_2N$), 7.45−7.54 (m, 4H, benzimidazolyl), 7.91 (d, $J$ = 8.0 Hz, 2H, benzimidazolyl), 8.22 (d, $J$ = 8.5 Hz, 2H, benzimidazolyl), 8.43 (t, $J$ = 8.0 Hz, 1H, pyridyl), 8.79 ppm (d, $J$ = 8.4 Hz, 2H, pyridyl). Negative FAB MS: $m/z$: 784 [M − K]$^-$. Elemental analysis calcd (%) for $C_{25}H_{23}ClKN_5O_6PtS_2\cdot 1.5H_2O$: C, 35.31; H, 3.08; N, 8.23; found: C, 35.48; H, 2.87; N, 7.99.

*Synthesis of **1**·PPN.* **1**·PPN was prepared by metathesis reaction of **1**·K. A saturated aqueous solution of PPNCl was added dropwise to a warm solution of **1**·K in $H_2O$. The deep-blue precipitate was collected by filtration. Subsequent recrystallization of the precipitate by the slow diffusion of diethyl ether vapor into a dichloromethane solution of the metathesized product yielded the pure product. $^1$H NMR (400 MHz, [$D_3$]MeCN, 343 K): $\delta$ 2.27 (m, 2H, $CH_2$), 2.83 (t, $J$ = 6.0 Hz, 2H, $CH_2SO_3$), 4.81 (t, 2H, $J$ = 8.5 Hz, $CH_2N$), 7.34 (t, $J$ = 7.5 Hz, 2H, benzimidazolyl), 7.44 (t, $J$ = 7.4 Hz, 2H, benzimidazolyl), 7.49−7.69 (m, 32H, benzimidazolyl and PPN), 8.06 (d, $J$ = 8.2 Hz, 2H, benzimidazolyl), 8.42 (t, $J$ = 8.2 Hz, 1H, pyridyl), 8.75 ppm (d, $J$ = 8.2 Hz, 2H, pyridyl). Negative FAB MS: $m/z$: 784 [M − PPN]$^-$. Elemental analysis calcd (%) for $C_{61}H_{53}ClN_6O_6P_2PtS_2\cdot 2CH_2Cl_2$: C, 50.70; H, 3.85; N, 5.63; found: C, 50.72; H, 4.00; N 5.85.

*Synthesis of **2**·K.* To a solution of **1**·PPN (0.30 g, 0.22 mmol) in degassed 100 mL $CH_2Cl_2$ were added tri-*n*-octylamine (1 mL), TMS−C≡C−C≡CH (0.08 g, 0.68 mmol) and a catalytic amount of CuI. The reaction mixture was allowed to stir under $N_2$ atmosphere at room temperature until the reaction was complete. After removal of solvents, the solid was washed with diethyl ether, and methanol was then added to dissolve the solid. After filtration, an acetonitrile solution of $KPF_6$ was added to the solution for the metathesis reactions to yield orange solids of the pure product. Yield: 0.17 g (81%). $^1$H NMR (400 MHz, [$D_6$]DMSO, 298 K): $\delta$ 0.31 (s, 9H, $SiMe_3$), 2.21 (m, 2H, $CH_2$), 2.68 (t, $J$ = 6.0 Hz, 2H, $CH_2SO_3$), 4.92 (t, 2H, $J$ = 7.2 Hz, $CH_2N$), 7.46−7.54 (m, 4H, benzimidazolyl), 7.87 (d, $J$ = 7.0 Hz, 2H, benzimidazolyl), 7.92 (d, $J$ = 8.2 Hz, 2H, benzimidazolyl), 8.39 (t, $J$ = 8.2 Hz, 1H, pyridyl), 8.85 ppm (d, $J$ = 8.4 Hz, 2H, pyridyl). IR (KBr): $\nu$ = 2187 (w; $\nu$(C≡C)), 2132 cm$^{-1}$ (w; $\nu$(C≡C)); Negative FAB MS: $m/z$: 869 [M − K]$^-$. Elemental analysis calcd (%) for $C_{32}H_{32}KN_5O_6PtS_2Si\cdot H_2O$: C, 41.46; H, 3.70; N, 7.55; found: C, 41.50; H, 3.59; N, 7.59.

*Synthesis of **3**·K.* To a solution of **2**·K (0.14 g, 0.15 mmol) in $H_2O$ was added $K_2CO_3$ (0.14 g, 1 mmol) to give a red solution. The solution was allowed to stir under a $N_2$ atmosphere at room temperature for 2 h. PPNCl was added to precipitate out the metathesized product. After filtration, the red solid was redissolved in $CH_2Cl_2$, and an acetonitrile solution of $KPF_6$ was added to give **3**·K as a red solid. Yield: 0.11 g (90%). $^1$H NMR (400 MHz, [$D_6$]DMSO, 298 K): $\delta$ 2.20 (m, 2H, $CH_2$), 2.69 (t, $J$ = 5.8 Hz, 2H, $CH_2SO_3$), 2.97 (s, 1H, C≡CH), 4.86 (t, 2H, $J$ = 7.0 Hz, $CH_2N$), 7.41−7.49 (m, 4H, benzimidazolyl), 7.84−7.86 (m, 4H, benzimidazolyl), 8.44 (t, $J$ = 8.0 Hz, 1H, pyridyl), 8.88 ppm (d, $J$ = 8.2 Hz, 2H, pyridyl). IR (KBr): $\nu$ = 2152 cm$^{-1}$ (w; $\nu$(C≡C)); Negative FAB MS: $m/z$: 797 [M − K]$^-$. Elemental analysis calcd (%) for $C_{29}H_{24}KN_5O_6PtS_2\cdot 2.5CH_2Cl_2$: C, 36.06; H, 2.79; N, 6.68; found: C, 35.73; H, 2.72; N, 6.97.

*Physical Measurements and Instrumentation.* $^1$H NMR spectra were recorded on a Bruker AVANCE 400 (400 MHz) Fourier-transform NMR spectrometer with chemical shifts reported relative to tetramethylsilane, $(CH_3)_4Si$. Negative-ion FAB mass spectra were recorded on a Thermo Scientific DFS high resolution magnetic sector mass spectrometer. IR spectra were obtained as KBr disk on a Bio-Rad FTS-7 Fourier transform infrared spectrophotometer (4000−400 cm$^{-1}$). Elemental analyses of complexes were preformed on a Flash EA 1112 elemental analyzer at the Institute of Chemistry, Chinese Academy of Sciences. The UV−visible spectra were obtained using a Hewlett-Packard 8452A diode array spectrophotometer. Steady-state excitation and emission spectra at room temperature and at 77 K were recorded on a Spex Fluorolog-3 model FL3-211 fluorescence spectrofluorometer equipped

with an R2658P PMT detector. Variable-temperature UV−vis absorption and emission spectra were obtained using a Varian Cary 50 UV−vis spectrophotometer and a Spex Fluorolog-3 model FL3-211 fluorescence spectrofluorometer equipped with an R2658P PMT detector, respectively. Solid-state photophysical studies were carried out with solid samples contained in a quartz tube inside a quartz-walled Dewar flask. Measurements of solid-state sample at 77 K were similarly conducted with liquid nitrogen filled into the optical Dewar flask. As the yellow form of **1**·K is very hygroscopic, the absorption and emission measurements were carried out by suspending the solid in acetone to minimize the contact of moisture from the air during the course of measurements. Emission lifetime measurements were performed using a conventional laser system. The excitation source used was the 355-nm output (third harmonic) of a Spectra-Physics Quanta-Ray Q-switched GCR-150-10 pulsed Nd:YAG laser. Luminescence decay signals were detected by a Hamamatsu R928 PMT, recorded on a Tektronix model TDS-620A (500 MHz, 2 GS/s) digital oscilloscope, and analyzed using a program for exponential fits. Photoluminescence quantum yields were measured at room temperature by the optical dilute method reported by Demas and Crosby[26] using a degassed aqueous solution of $[Ru(bpy)_3]Cl_2$ (excitation wavelength = 436 nm, $\Phi = 0.042$) as reference.[27] All solutions for emission lifetime and luminescence quantum yield studies were degassed on a high-vacuum line in a two-compartment cell consisting of a 10-mL Pyrex bulb and a 1-cm path length quartz cuvette and sealed from the atmosphere by a Bibby Rotaflo HP6 Teflon stopper. The solutions were rigorously degassed with at least four successive freeze−pump−thaw cycles.

*Microscopy Studies.* Transmission electron microscopy (TEM) experiments were performed on a Philips Tecnai G2 20 S-TWIN transmission electron microscope with an accelerating voltage of 200 kV. The TEM images were taken by Gatan MultiScan model 794. The TEM samples were prepared by dropping a few drops of $10^{-4}$ M solution onto a carbon-coated copper grid. Scanning electron microscope (SEM) experiments were performed on a LEO 1530 FEG scanning electron microscope. Confocal fluorescence microcopy imaging experiments were performed on a Leica SPE laser confocal scanning microscope using a solid-state laser with excitation wavelengths of 405 nm and the emission spectrum was recorded by a Leica TCS SP5 laser confocal scanning microscope using a 488 nm laser. The solution samples were dropped onto microscopic slides, covered with coverslips, and then sealed from the atmosphere to prevent evaporation of the solvent.

*The Dimerization Plot for a Monomer−Dimer Equilibrium.* $K_{MM}$ and $K_{\pi\pi}$ for complex **1**·K in water were determined in the concentration range of $2.05 \times 10^{-6}$ to $8.26 \times 10^{-3}$ M using the equation[4c] shown below,

$$\frac{[Pt]}{\sqrt{A}} = \frac{1}{\sqrt{\varepsilon_{MM} K_{MM}}} + \left(\frac{2}{\varepsilon_{MM}} + \frac{2K_{\pi\pi}}{\varepsilon_{MM} K_{MM}}\right)\sqrt{A}$$

where [Pt] is the concentration, $A$ is the absorbance at a particular wavelength, $\varepsilon_{MM}$ is the extinction coefficient of the MMLCT band due to aggregation via metal−metal interactions and is taken to be 1350 $M^{-1}$ $cm^{-1}$ as determined from the UV−vis absorption studies. $K_{MM}$ and $K_{\pi\pi}$ are the equilibrium constants of dimerization due to metal−metal interactions and $\pi-\pi$ interactions respectively by assuming that there are two dimerization processes as shown below:

$$2Pt \overset{K_{\pi\pi}}{\rightleftharpoons} (Pt_2)_{\pi\pi}$$

$$2Pt \overset{K_{MM}}{\rightleftharpoons} (Pt_2)_{MM}$$

## ■ ASSOCIATED CONTENT

**Supporting Information.** UV−vis absorption and emission spectra of **2**·K and **3**·K in water−acetone mixture. $^1$H NMR spectra of **2**·K in various water−acetone compositions. SEM images of **1**·K and **2**·K prepared from 90% acetone−water mixture. Emission spectrum of luminescent rod recorded from the confocal fluorescence microscope. UV−vis absorption spectra **1**·K in water−THF, water−acetone, water−ethanol, and water−acetonitrile mixtures. This material is available free of charge via the Internet at http://pubs.acs.org.

## ■ AUTHOR INFORMATION

**Corresponding Author**
wwyam@hku.hk

## ■ ACKNOWLEDGMENT

V.W.-W.Y. acknowledges receipt of the Distinguished Research Achievement Award from The University of Hong Kong and the URC Strategic Research Theme on Molecular Materials. This work has been supported by the University Grants Committee Areas of Excellence Scheme (AoE/P-03/08) and the Research Grants Council of Hong Kong Special Administrative Region, China (HKU 7063/10P). C.P. acknowledges the receipt of a postgraduate studentship and a University Postgraduate Fellowship, and A.Y.-Y.T. the receipt of a University Postdoctoral Fellowship, both from The University of Hong Kong.

## ■ REFERENCES

(1) (a) Houlding, V. H.; Miskowski, V. M. *Coord. Chem. Rev.* **1991**, *111*, 145–152. (b) Miskowski, V. M.; Houlding, V. H. *Inorg. Chem.* **1989**, *28*, 1529–1533. (c) Miskowski, V. M.; Houlding, V. H. *Inorg. Chem.* **1991**, *30*, 4446–4452. (d) Biedermann, J.; Gliemann, G.; Klement, U.; Range, K. J.; Zabel, M. *Inorg. Chem.* **1990**, *29*, 1884–1888. (e) Connick, W. B.; Geiger, D.; Eisenberg, R. *Inorg. Chem.* **1999**, *38*, 3264–3265.

(2) (a) Connick, W. B.; Henling, L. M.; Marsh, R. E.; Gray, H. B. *Inorg. Chem.* **1996**, *35*, 6262–6265. (b) Connick, W. B.; Marsh, R. E.; Schaefer, W. P.; Gray, H. B. *Inorg. Chem.* **1997**, *36*, 913–922. (c) Herber, R. H.; Croft, M.; Coyer, M. J.; Bilash, B.; Sahiner, A. *Inorg. Chem.* **1994**, *33*, 2422–2426.

(3) (a) Eryazici, I.; Moorefield, C. N.; Newkome., G. R. *Chem. Rev.* **2008**, *108*, 1834–1895. (b) Yip, H. K.; Cheng, L. K.; Cheung, K. K.; Che, C. M. *J. Chem. Soc., Dalton Trans.* **1993**, 2933–2938. (c) Bailey, J. A.; Hill, M. G.; Marsh, R. E.; Miskowski, V. M.; Schaefer, W. P.; Gray, H. B. *Inorg. Chem.* **1995**, *34*, 4591–4599. (d) Aldridge, T. K.; Stacy, E. M.; McMillin, D. R. *Inorg. Chem.* **1994**, *33*, 722–727. (e) Arena, G.; Calogero, G.; Campagna, S.; Scolaro, L. M.; Ricevuto, V.; Romeo, R. *Inorg. Chem.* **1998**, *37*, 2763–2769. (f) Lai, S. W; Chan, M. C. W.; Cheung, K. K.; Che, C. M. *Inorg. Chem.* **1999**, *38*, 4262–4267. (g) Yam, V. W. W.; Tang, R. P. L.; Wong, K. M. C; Cheung, K. K. *Organometallics* **2001**, *20*, 4476–4482. (h) Büchner, R.; Cunningham, C. T.; Field, J. S.; Haines, R. J.; McMillin, D. R.; Summerton, G. C. *J. Chem. Soc., Dalton Trans.* **1999**, 711–718. (i) Wadas, T. J.; Wang, Q. M.; Kim, Y.; Flaschenreim, C.; Blanton, T. N.; Eisenberg, R. *J. Am. Chem. Soc.* **2004**, *126*, 16841–16849. (j) Jennette, K. W.; Lippard, S. J.; Vassiliades, G. A.; Bauer, W. R. *Proc. Natl. Acad. Sci. U.S.A.* **1974**, *71*, 3839–3843.

(4) (a) Jennette, K. W.; Gill, J. T.; Sadownick, J. A.; Lippard, S. J. *J. Am. Chem. Soc.* **1976**, *98*, 6159–6168. (b) Hill, M. G.; Bailey, J. A.; Miskowski, V. M.; Gray, H. B. *Inorg. Chem.* **1996**, *35*, 4585–4590. (c) Bailey, J. A.; Hill, M. G.; Marsh, R. E.; Miskowski, V. M.; Schaefer, W. P.; Gray, H. B. *Inorg. Chem.* **1995**, *34*, 4591–4599. (d) Wong, K. M. C.; Zhu, N.; Yam, V. W. W. *Chem. Commun.* **2006**, 3441–3443. (e) Lu, W.; Chan, M. C. W.; Zhu, N.; Che, C. M.; Li, C.; Hui, Z. *J. Am.*

*Chem. Soc.* **2004**, *126*, 7639–7651. (f) Lu, W.; Chen, Y.; Roy, V. A. L.; Chui, S. S. Y.; Che, C. M. *Angew. Chem., Int. Ed.* **2009**, *48*, 7621–7625. (g) Chen, Y.; Li, K.; Lu, W.; Chui, S. S. Y.; Ma, C. W.; Che, C. M. *Angew. Chem., Int. Ed.* **2009**, *48*, 9909–9913.

(5) (a) Yam, V. W. W.; Wong, K. M. C.; Zhu, N. Y. *J. Am. Chem. Soc.* **2002**, *124*, 6506–6507. (b) Yam, V. W. W.; Chan, K. H. Y.; Wong, K. M. C.; Zhu, N. *Chem.—Eur. J.* **2005**, *11*, 4535–4543 ($PttpyC_4H$).

(6) (a) Yam, V. W. W.; Chan, K. H. Y.; Wong, K. M. C.; Chu., B. W. K. *Angew. Chem., Int. Ed.* **2006**, *45*, 6169–6173. (b) Chan, K. H. Y.; Chow, H. S.; Wong, K. M. C.; Yeung, M. C. L.; Yam, V. W. W. *Chem. Sci.* **2010**, *1*, 477–482.

(7) (a) Tam, A. Y. Y.; Wong, K. M. C.; Wang, G.; Yam, V. W. W. *Chem. Commun.* **2007**, 2028–2030. (b) Tam, A. Y. Y.; Wong, K. M. C.; Yam, V. W. W. *Chem.—Eur. J.* **2009**, *15*, 4775–4778. (c) Tam, A. Y. Y.; Wong, K. M. C.; Zhu, N.; Wang, G.; Yam, V. W. W. *Langmuir* **2009**, *25*, 8685–8695.

(8) (a) Yam, V. W. W.; Hu, Y. C.; Chan, K. H. Y.; Chung, C. Y. S. *Chem. Commun.* **2009**, 6216–6218. (b) Yu, C.; Wong, K. M. C.; Chan, K. H.Y.; Yam, V. W. W. *Angew. Chem., Int. Ed.* **2005**, *44*, 791–794. (c) Yu, C.; Chan, K. H. Y.; Wong, K. M. C.; Yam, V. W. W. *Chem. —Eur. J.* **2008**, *14*, 4577–4584. (d) Chung, C. Y. S.; Chan, K. H. Y.; Yam, V. W. W. *Chem. Commun.* **2011**, *47*, 2000–2002.

(9) (a) Yu, C.; Chan, K. H. Y.; Wong, K. M. C.; Yam, V. W. W. *Proc. Natl. Acad. Sci. U.S.A.* **2006**, *103*, 19652–19657. (b) Yu, C.; Chan, K. H. Y.; Wong, K. M. C.; Yam, V. W. W. *Chem. Commun.* **2009**, 3756–3758. (c) Yeung, M. C. L.; Wong, K. M. C.; Tsang, Y. K. T.; Yam, V. W. W. *Chem. Commun.* **2010**, *46*, 7709–7711.

(10) Mann, K. R.; Gordon, J. G., II; Gray, H. B. *J. Am. Chem. Soc.* **1975**, *97*, 3553–3555.

(11) (a) Grove, L. J.; Rennekamp, J. M.; Jude, H.; Connick, W. B. *J. Am. Chem. Soc.* **2004**, *126*, 1584–1595. (b) Grove, L. J.; Oliver, A. G.; Krause, J. A.; Connick, W. B. *Inorg. Chem.* **2008**, *47*, 1408–1410.

(12) Wang, K.; Haga, M.; Monjushiro, H.; Akiba, M.; Sasaki, Y. *Inorg. Chem.* **2000**, *39*, 4022–4028.

(13) (a) Tam, A. Y. Y.; Lam, W. H.; Wong, K. M. C.; Zhu, N.; Yam, V. W. W. *Chem.—Eur. J.* **2008**, *14*, 4562–4576. (b) Tam, A. Y. Y.; Wong, K. M. C.; Yam, V. W. W. *J. Am. Chem. Soc.* **2009**, *131*, 6253–6260.

(14) (a) Lehn, J. M. *Supramolecular Chemistry: Concepts and Perspectives*; VCH: Weinheim, Germany, **1995**. (b) Terech, P.; Weiss, R. G. *Chem. Rev.* **1997**, *97*, 3133–3159. (c) Hoeben, F. J. M.; Jonkheijm, P.; Meijer, E. W.; Schenning, A. P. H. J. *Chem. Rev.* **2005**, *105*, 1491–1546. (d) Ajayaghosh, A.; Praveen, V. K.; Vijayakumar, C. *Chem. Soc. Rev.* **2008**, *37*, 109–122. (e) Elemans, J. A. A. W.; van Hameren, R.; Nolte, R. J. M.; Rowan, A. E. *Adv. Mater.* **2006**, *18*, 1251–1266. (f) Lehn, J. M. *Science* **2002**, *295*, 2400–2403.

(15) (a) Zhang, L. F.; Eisenberg, A. *Science* **1995**, *268*, 1728–1731. (b) Zhang, L. F.; Yu, K.; Eisenberg, A. *Science* **1996**, *272*, 1777–1779.

(16) (a) van Hest, J. C. M.; Delnoye, D. A. P; Baars, M.W. P. L.; van Genderen, M. H. P.; Meijer, E. W. *Science* **1995**, *268*, 1592–1595. (b) Choucair, A.; Eisenberg, A. *Eur. Phys. J. E* **2003**, *10*, 37–44. (c) Verma, S.; Hauck, T.; Khouly, M. E. E.; Padmawar, P. A.; Canteenwala, T.; Pritzker, K.; Ito, O.; Chiang, L. Y. *Langmuir* **2005**, *21*, 3267–3272.

(17) (a) Discher, D. E.; Eisenberg, A. *Science* **2002**, *297*, 967–973. (b) Discher, D. E.; Ortizb, V.; Srinivasb, G.; Kleinb, M. L.; Kima, Y.; Christiana, D.; Caia, S.; Photosa, P.; Ahmed, F. *Prog. Polym. Sci.* **2007**, *32*, 838–857. (c) Yan, X.; He, Q.; Wang, K.; Duan, L.; Cui, Y.; Li, J. *Angew. Chem., Int. Ed.* **2007**, *46*, 2431–2434.

(18) (a) Seo, S. H.; Chang, J. Y.; Tew, G. N. *Angew. Chem., Int. Ed.* **2006**, *45*, 7526–7530. (b) Hill, J. P.; Jin, W.; Kosaka, A.; Fukushima, T.; Ichihara, H.; Shimomura, T.; Ito, K.; Hashizume, T.; Ishii, N.; Aida, T. *Science* **2004**, *304*, 1481–1483. (c) Wu, J.; Li, J.; Kolb, U.; Müllen, K. *Chem. Commun.* **2006**, 48–50. (d) Feng, X.; Pisula, W.; Kudernac, T.; Wu, D.; Zhi, L.; Feyter, S.; de; Müllen, K. *J. Am. Chem. Soc.* **2009**, *131*, 4439–4448. (e) Zhang, X.; Chen, Z.; Würthner, F. *J. Am. Chem. Soc.* **2007**, *129*, 4886–4887. (f) Rao, K. V.; George, S. J. *Org. Lett.* **2010**, *12*, 2656–2659. (g) Jiang, B. P.; Guo, D. S.; Liu, Y. *J. Org. Chem.* **2010**, *75*, 7258–7264. (h) Zhang, X.; Wang, C. *Chem. Soc. Rev.* **2011**, *40*, 94–101.

(19) (a) Yagai, S.; Nakano, Y.; Seki, S.; Asano, A.; Okubo, T.; Isoshima, T.; Karatsu, T.; Kitamura, A.; Kikkawa, Y. *Angew. Chem., Int. Ed.* **2010**, *49*, 9990–9994. (b) Jiang, B. P.; Guo, D. S.; Liu, Y. *J. Org. Chem.* **2010**, *75*, 7258–7264.

(20) (a) Sprintschnik, G.; Sprintschnik, H. W.; Kirsch, P. P.; Whitten, D. G. *J. Am. Chem. Soc.* **1976**, *98*, 2337–2338. (b) Sprintschnik, G.; Sprintschnik, H. W.; Kirsch, P. P.; Whitten, D. G. *J. Am. Chem. Soc.* **1977**, *99*, 4947–4954. (c) Golubkov, G.; Weissman, H.; Shirman, E.; Wolf, S. G.; Pinkas, I.; Rybtchinski, B. *Angew. Chem., Int. Ed.* **2009**, *48*, 926–930. (d) Gohy, J. F.; Lohmeijer, B. G. G.; Schubert, U. S. *Macromolecules* **2002**, *35*, 4560–4563. (e) Gohy, J. F.; Lohmeijer, B. G. G.; Varshney, S. K.; Décamps, B.; Leroy, E; Boileau, S.; Schubert, U. S. *Macromolecules* **2002**, *35*, 9748–9755. (f) Song, B.; Wu, G.; Wang, Z.; Zhang, X. *Langmuir* **2009**, *25*, 13306–13310. (g) Chen, Y.; Li, K.; Lloyd, H. O.; Lu, W.; Chui, S. S. Y.; Che, C. M. *Angew. Chem., Int. Ed.* **2010**, *49*, 9968–9971. (h) Kishimura, Al; Yamashita, T.; Aida, T. *J. Am. Chem. Soc.* **2005**, *127*, 179–183.

(21) (a) Zhao, L.; Wong, K. M. C.; Li, B.; Li, W.; Zhu, N.; Wu, L.; Yam, V. W. W. *Chem.—Eur. J.* **2010**, *16*, 6797–6809. (b) Lam, S. T.; Wang, G.; Yam, V. W. W. *Organometallics* **2008**, *27*, 4545–4548. (c) Zhang, J.; Chu, B. W. K.; Zhu, N.; Yam, V. W. W. *Organometallics* **2007**, *26*, 5423–5429. (d) Chu, B. W. K.; Yam, V. W. W. *Langmuir* **2006**, *22*, 7437–7443. (e) Yam, V. W. W.; Li, B.; Zhu, N. *Adv. Mater.* **2002**, *14*, 719–722.

(22) Mann, K. R.; Roger, N. L.; Williams, M.; Gray, H. B.; Gordon, J. G., II. *Inorg. Chem.* **1978**, *17*, 828–834.

(23) (a) Chandrasekhar, V.; Boomishankar, R.; Steiner, A.; Bickley, J. F. *Organometallics* **2003**, *22*, 3342–3344. (b) Russell, V. A.; Etter, M. C.; Ward, M. D. *J. Am. Chem. Soc.* **1994**, *116*, 1941–1952.

(24) Aizpurua, J. M.; Azcune, I.; Fratila, R. M.; Balentova, E.; Sagartzazu-Aizpurua, M.; Miranda, J. I. *Org. Lett.* **2010**, *12*, 1584–1587.

(25) Addison, A. W.; Burke, P. J. *J. Heterocycl. Chem.* **1981**, *18*, 803–805.

(26) Demas, J. N.; Crosby, G. A. *J. Phys. Chem.* **1971**, *75*, 991–1024.

(27) Van Houten, J.; Watts, R. *J. Am. Chem. Soc.* **1976**, *98*, 4853–4858.